Behavioral oscillation in global/local processing: Global alpha oscillations mediate global precedence effect

Ling Liu

School of Psychological and Cognitive Sciences, Peking University, Beijing, China
McGovern Institute for Brain Research, Peking University, Beijing, China
Beijing Key Laboratory of Behavior and Mental Health, Peking University, Beijing, China

Huan Luo

School of Psychological and Cognitive Sciences, Peking University, Beijing, China
McGovern Institute for Brain Research, Peking University, Beijing, China
Beijing Key Laboratory of Behavior and Mental Health, Peking University, Beijing, China

A visual scene always contains hierarchically organized structures, and determining how the brain coordinates the processing of global and local features is thus central for understanding visual perception. Recent neuroimaging studies have shown that global/local analyses are separately mediated through neuronal oscillations at different frequencies. However, it remains unclear how these rhythmic profiles are associated with and contribute to the global precedence effect (GPE) , the classical finding that global properties are perceived faster than local ones. Here, by using a time-resolved psychophysical method, we demonstrate that the global/local behavioral traces consist of two temporal components: one that resembles the classic GPE and one that manifests oscillatory pattern. Specifically, these behavioral oscillations occur in the alpha-band (~10 Hz) and beta-band (~20 Hz) for global and local tasks respectively ("Global-alpha" and "Local-beta"). Importantly, subjects with stronger Global-alpha not only show larger GPE but also are less vulnerable to local interference. Together, these findings constitute novel behavioral evidence supporting the idea that neuronal oscillations at different frequencies mediate and coordinate the global/local analysis of visual inputs and further reveal the possible neural basis underlying global precedence.

Introduction

A visual scene typically involves a set of hierarchically organized features, from local to global ones. How our brain processes and coordinates these features together is a fundamental question in vision research. The classical stimulus used to examine the global/local processing is the Navon stimulus (Navon, 1977), a type of hierarchical compound stimulus containing global and local features, both of which could be flexibly and precisely manipulated and combined. For example, the global shape of the compound stimulus could be a big letter-like figure, which is further composed of small letter-like figures. Subjects are then instructed to perceive either the global or local attributes of the compound stimulus, and their performance could be examined as performance for global or local processing. It is well established in behavioral studies that global properties are perceived faster than local features, a phenomenon termed global precedence effect (GPE; Navon, 1977).

Recent neuroimaging studies have shown that global and local operations are linked to neuronal oscillations at different frequencies (Romei, Driver, Schyns, & Thut, 2011; Romei, Thut, Mok, Schyns, & Driver, 2012; Smith, Gosselin, & Schyns, 2006). For example, in one EEG study (Smith et al., 2006), subjects were presented with an ambiguous visual stimulus, the perception of which could be biased toward either global level or local level. It was found that the subjects' global/local reporting was strongly correlated with the theta-band (4–8 Hz) and beta-band (12–25 Hz) neuronal responses at parietal electrodes respectively. Moreover, a transcranial

Citation: Liu, L., & Luo, H. (2019). Behavioral oscillation in global/local processing: Global alpha oscillations mediate global precedence effect. *Journal of Vision*, *19*(5):12, 1–12, https://doi.org/10.1167/19.5.12.

https://doi.org/10.1167/19.5.12 Received October 23, 2018; published May 17, 2019 ISSN 1534-7362

magnetic stimulation (TMS) study provided further causal evidence for the frequency-based dissociation for global and local perception. Specifically, short rhythmic bursts of right-parietal TMS at theta/alpha or beta frequency can benefit processing of global or local features respectively (Romei et al., 2011; Romei et al., 2012). Furthermore, global perception is related to theta-band and alpha-band neuronal responses that originate from parietal-occipital and occipital channels respectively (Flevaris, Bentin, & Robertson, 2011). Taken together, these results consistently suggest that global and local properties are separately mediated via low-frequency (i.e., theta/alpha-band) and high-frequency (i.e., beta band) neuronal oscillations. However, it remains largely unknown how the global/local neuronal oscillations are linked to and engage in the aforementioned GPE (i.e., the speedy processing of the global features compared to local ones).

A series of recent behavioral studies have provided new insights and tools to address the relationship between the classical effect and the neural oscillations. Specifically, by employing a time-resolved behavioral measurement (Drewes, Zhu, Wutz, & Melcher, 2015; Fiebelkorn et al., 2011; Fiebelkorn, Pinsk, & Kastner, 2018; Fiebelkorn, Saalmann, & Kastner, 2013; Huang, Chen, & Luo, 2015; Landau & Fries, 2012; Song, Meng, Chen, Zhou, & Luo, 2014; Tomassini, Ambrogioni, Medendorp, & Maris, 2017; Tomassini, Spinelli, Jacono, Sandini, & Morrone, 2015; Wang & Luo, 2017), which was manipulated in a cue-target design with a time-resolved measurements aligned to the cue, several studies have revealed, within the same behavioral time courses, a classical behavioral profile represented in slow trends and additional neurophysiological-relevant oscillatory components (Fiebelkorn et al., 2013; Huang et al., 2015; Song et al., 2014). Motivated by these findings, here we used the time-resolved behavioral approach to examine the fine temporal structure of behavioral time courses in global/local analysis of hierarchical compound visual stimulus. In addition to expecting to replicate the classical GPE in the slow trends of the time-resolved behavioral courses, we are mainly interested in investigating two unclear issues. First, could we reveal dissociated oscillatory components for global and local processing, which have only been previously demonstrated in neurophysiological recordings, in behavioral performance directly? Second, if we indeed observed behavioral rhythmic profiles, we would further examine the associations between the global/local behavioral oscillations and the GPE to understand how oscillations engage in the global/local analysis.

Materials and methods

Subjects

Twenty-six human subjects (ten males, 16 females, right-handed, mean age = 23 years, normal or corrected-to-normal vision) participated in the experiment. All subjects had normal or corrected-to-normal visual acuity and provided informed consent. The study was approved by the ethics committee of Peking University, Beijing (2015-03-05c2). They were paid as compensation for their time. One subject was excluded from further analysis because of the poor performance. The sample size was chosen based on previous global/local perception experiments (Flevaris et al., 2011) as well as previous behavior oscillation experiments (Fiebelkorn et al., 2013; Huang et al., 2015; Landau & Fries, 2012). Moreover, we calculated the power of the main results in the current experiment (power > 0.94).

Experimental procedures

Subjects sat in a dark room 57 cm in front of a gamma-corrected CRT monitor (100 Hz), and their responses were recorded using a push-button response box (CB6, Cambridge Research Systems). Visual stimuli were generated by the visual stimulator (ViSaGe MKII, Cambridge Research System). The stimulus was black (0 cd/m2) and the background was gray (181 cd/m2). The target stimulus was a hierarchical visual stimuli, containing a big arrow figure (pointing left or right, global property, $6.36° \times 2.58°$) being composed of small arrow figures (pointing left or right, local property, $0.55° \times 0.39°$). The global and local properties were either congruent or incongruent with each other.

As shown in Figure 1, in each trial, after 200 ms, a cue ('global' or 'local' in text) was presented for 100 ms to instruct subjects which feature of the subsequently presented compound visual stimulus they should attend to and report. Specifically, subjects were instructed to determine the orientation (left or right) of the global or local property of the target compound stimulus, according to the initially presented cue (Chinese character "大": reporting global feature; Chinese character "小": reporting local feature), and their reaction time (RT) was recorded as a behavioral measurement. Participants were instructed to maintain central fixation throughout the whole experiment. Critically, here we employed a time-resolved behavioral measurement to achieve a dense temporal assessment of the behavioral performance. Specifically, the target stimulus could appear at one of 50 temporal intervals, in step of 10 ms, from 110 to 600 ms after cue onset. Each subject completed 1,600 trials in total, in 4 blocks

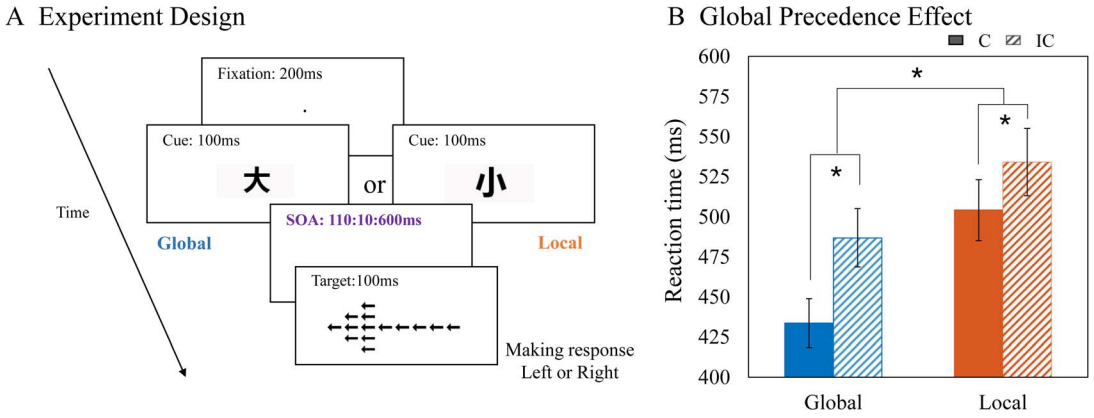

Figure 1. Experiment paradigm and global precedence effect. (A) Subjects were instructed to fix at a central cross and make speeded responses to report either the global (G) or local (L) orientation of a compound target stimulus (pointing left or right), according to an initially presented instruction cue (Chinese character "大": global property; Chinese character "小": local property). The global and local properties were either congruent (C) or incongruent (IC) with each other. The trial sequence consisted of a 200 ms fixation screen, a 100 ms cue stimulus, and a 100 ms compound target stimulus. Notably, the target stimulus occurred at varying intervals (SOA: 110 ms to 600 ms in steps of 10 ms) after the onset of the cue stimulus. (B) Grand average ($n = 25$, mean ± *SD*) reaction time (averaged across all SOAs) for four conditions (Global-congruent, 433.7 ± 15.2; Global-incongruent, 486.9 ± 18.9; Local-congruent, 504.1 ± 18.1; Local-incongruent, 534.1 ± 21.0).

interleaved with a 5-min break. Each block lasted around 15 min. The cue-to-target SOA of each trial was pseudorandom from 110 to 600 ms, balanced across trials to have the exact same likelihood. To further increase the signal-to-noise ratio of the behavioral time courses, we employed a previous approach (Fiebelkorn et al., 2013) to smooth the RT time courses by averaging RTs across consecutive 2 SOAs.

Data analysis

The behavioral RT data was analyzed with MATLAB (MathWorks, Natick, MA; RRID: SCR_001622). For each subject, trials with either RTs that were > 4 *SD*s across all trials or incorrect answers were excluded from further analysis. To examine the classical global precedence effect (GPE) and interference effect (IE), we averaged the RTs across all SOAs for each condition separately (global/local and congruent/incongruent). The GPE was calculated as the RT difference between local and global task. The IE was calculated as the RT difference between incongruent and congruent conditions for global and local tasks separately.

RTs were first normalized within each subject separately. Specifically, for each subject, RTs for all trials (i.e., all conditions) were pooled together to do the normalization, from which the z score for RT in each trial was obtained. To obtain the slow trend of the time-resolved behavioral traces, we first calculated the 100 ms moving average of the RT time courses for global and local conditions separately for each subject respectively. These slow trend signals were then subtracted from the corresponding time-resolved RT time courses to obtain the detrended RT time courses for each condition (Fiebelkorn et al., 2013; Huang et al., 2015; Song et al., 2014). Further analysis was then performed on the detrended RT time courses.

The detrended RT time courses were first pooled across all participants before spectrum analysis ("aggregate subject data analysis"), similar to previous behavioral oscillation studies (e.g., (Fiebelkorn et al., 2013; Ho, Leung, Burr, Alais, & Morrone, 2017; Landau & Fries, 2012). Spectral analysis was then performed on the aggregate subject data (the temporal profile from 110 to 600 ms) for the global and local task separately to assess their frequency profiles. The 490 ms time series was Hanning tapered, zero-padded, and Fourier transformed (FFT). The amplitude spectra were the absolute values of the Fourier spectra. We further performed a randomization procedure by shuffling the time points (permutation number = 2,000) on the detrended RT temporal profiles to assess statistical significance of the peaks found in the spectra amplitude (Fiebelkorn et al., 2013; Huang et al., 2015; Maris & Oostenveld, 2007; Song et al., 2014). In each iteration, time points were shuffled in each participant separately, and the shuffled time courses were then pooled across all participants as a new aggregate subject data. The same detrending as well as the spectra analyses were then performed on the shuffled time series and resulted in a distribution of 2,000 amplitude values for each frequency bin from which we could obtain the $p < 0.05$ threshold. The p values were further FDR corrected across frequencies (5–15 Hz for global task; 15–25 Hz for local task).

To further examine the robustness of the oscillatory profile in the data, a single-trial linear model approach (Tomassini, Ambrogioni, Medendorp, & Maris, 2017) was applied to the RT time courses for each subject. For each trial, the phase of the sinusoidal function at stimulus presentation time was computed as $2\pi \times f \times t$ (f: the sinusoidal frequency; t: stimulus presentation time relative to the cue onset). The sine and the cosine of the resulting phase value were then used as regressors (independent variables) to predict the perceptual performance (reaction times in each trial, dependent variables) in a regression analysis. Separate regression models were fitted for each subject and in each frequency ranging from 2 to 25 Hz. A group-level (random effects) analysis was then performed by testing the average of the participant-specific beta coefficients against zero, by means of the bivariate Hotelling's T-square statistics.

A correlation analysis was performed to examine the relationship between oscillation components (i.e., Global-alpha and Local-beta amplitude) and classical behavioral effect (i.e., GPE and IE). First, in each subject, we extract the alpha-band amplitude in the global condition ("Global-alpha") and beta-band amplitude in the local condition ("Local-beta"), and we then calculated the correlation (Pearson correlation) between the oscillation components (Global-alpha and Local-beta) and GPE score across subjects. Similar analysis was also performed to assess the relationship between oscillation and the IE score. Since the global-alpha was correlated with both GPE score and IE score, we also performed a mediation analysis (Hayes, 2018) to explore the connections across the three variables (i.e., Global-alpha, GPE, and IE).

To further determine the relationship between Global-alpha and GPE, we divided all the subjects into two subgroups based on their overall GPEs: high GPE group ($N = 12$) and low GPE group ($N = 12$). We next performed the same spectrum analyses on each group separately to examine their spectrum difference.

Results

As shown in Figure 1A, after a 200 ms central fixation, a cue (Chinese character "大": global; Chinese character "小": local) appeared on the screen to instruct subjects to report either the global or local property of a forthcoming compound target stimulus. The global/local compound target comprised Navon-type hierarchical structure (Navon, 1977) such that the global shape was a left- or right-pointing arrow, which further consisted of 14 small local arrow figures (left- or right-pointing). The global (G) and local (L) properties were either congruent (C) or incongruent (IC) with each other. Critically, to assess the fine temporal dynamics of global/local perception, we employed a time-resolved measurement by ranging the cue-to-target SOA from 0.11 s to 0.6 s in steps of 0.01 s. We then calculated the reaction time as a function of cue-to-target SOA for global and local conditions separately to examine the temporal course for global/local processing.

Global precedence effect (GPE) and interference effect (IE)

Twenty five subjects participated in the global/local task and performed well (Global task, hit rate: 0.971 ± 0.034, false alarm rates: 0.029 ± 0.034; Local task, hit rate: 0.968 ± 0.030, false alarm rate: 0.032 ± 0.030). Only trials with correct answers were included into further analysis. We first averaged the raw RTs across all the tested SOAs (0.11 ~ 0.6 s) to examine the overall behavioral performance for each of the four conditions (Global/local * C/IC) separately. As shown in Figure 1B, the overall behavioral performances replicated the classical global precedence effect (GPE) as well as the interference effect (IE) in global/local perception tasks (Navon, 1977). Specifically, global task (blue) showed shorter RTs than local task (red), and congruent condition (solid bar) showed shorter RTs than incongruent (checked bar) condition: two-way repeated ANOVA, main effect of GL: $F(1, 24) = 97.55$, $\eta^2 = 0.80$, $p < 0.001$; main effect of C/IC: $F(1, 24) = 73.70$, $\eta^2 = 0.75$, $p < 0.001$; interaction effect: $F(1, 24) = 11.50$, $\eta^2 = 0.32$, $p = 0.002$. Therefore, we replicated the classical GPE and IE in the present experiment.

Alpha/beta-band behavioral dynamics for global/local tasks Global-alpha and Local-beta

We next examined the fine temporal structure of the global/local RT course (pooling congruent and incongruent conditions to increase signal to noise ratios) for global and local tasks separately. Figure 2A plots the grand average RT time courses as a function of cue-to-target SOAs for global (blue) and local (red) tasks. The slow trends of the RT time courses were then extracted in each subject by calculating the 100 ms smoothed RT traces for the global and local conditions separately, which again showed a classical GPE and gradual RT declining profile (Figure 2B), suggesting the replication of classical behavioral effect in slow trends. Moreover, to avoid the interferences from the slow trends (Fiebelkorn et al., 2013; Huang et al., 2015; Song et al., 2014), we subtracted them from the raw RT courses separately for each subject, resulting in the detrended behavioral courses for global (blue) and local (red)

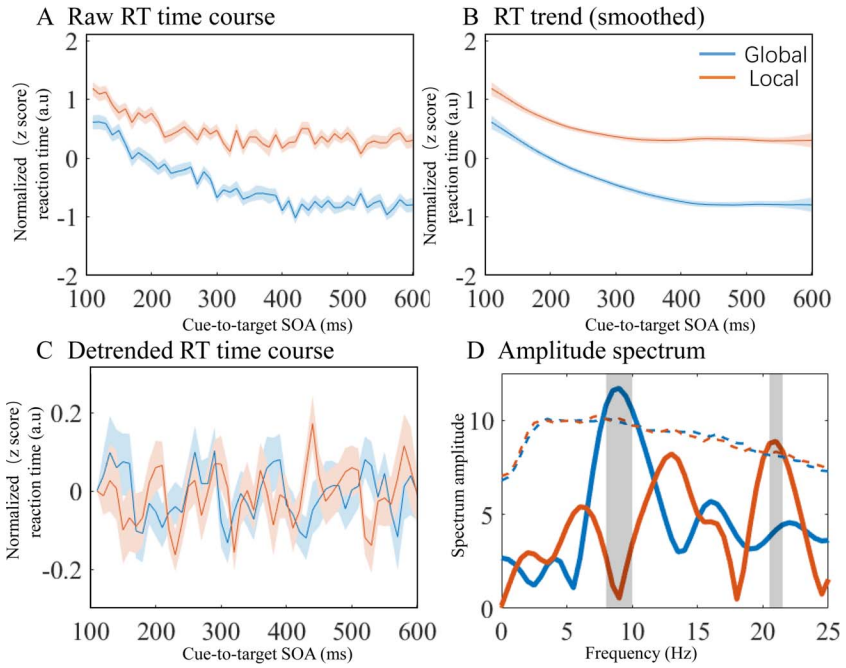

Figure 2. Slow trend, Global-alpha, and Local-beta. (A) Grand average reaction time (RT) time courses ($n = 25$) as a function of cue-to-target SOA (100–600 ms), for global (blue) and local (red) tasks. (B) Grand average 100 ms smoothed RT time courses representing slowly developing trends, which resemble the classical global precedence effects, for global (blue) and local (red) tasks. (C) Grand average detrended RT time courses as a function of cue-to-target SOA (100–600 ms) for global (blue) and local (red) tasks. (D) Amplitude spectrum for the detrended RT time courses as a function of frequency from 0 to 25 Hz, for global (blue) and local (red) tasks. The dashed lines represent the permutation test threshold (permutation test, $p < 0.05$) for global (blue) and local (red) conditions respectively. Gray shades mark the significant frequency range for global and local processing respectively ("Global-alpha" and "Local-beta").

tasks (Figure 2C). Similar results were obtained when using a polynomial fitting approach to extract slow trends (Supplementary Figure S1).

To examine the characteristics of oscillatory components in global and local conditions, we performed spectrum analyses on the detrended time traces (see the raw RT spectrum in Supplementary Figure S2). In addition, to test whether they might simply reflect random temporal fluctuations, a permutation test (Fiebelkorn et al., 2013; Huang et al., 2015; Song et al., 2014) was used to examine the statistical significances. Figure 2D illustrates the amplitude spectrum of the detrended RT traces for the global (blue) and local (red) conditions. Interestingly, global task (blue) showed significant activations in the alpha-band (8–10 Hz, permutation test, $p = 0.013$, FDR corrected), whereas local task (red) displayed beta-band activations (~20 Hz, permutation test, $p = 0.041$, uncorrected). Results based on median of RTs showed similar pattern (Supplementary Figure S3). To further examine the robustness of the results, a single trial fitting approach (Tomassini, Ambrogioni, Medendorp, & Maris, 2017), which was independent of calculating mean or median values of RTs, was applied to the detrended RTs, and the similar "Global-alpha" ($p = 0.021$, uncorrected) and "Local-beta" ($p = 0.056$, uncorrected) pattern was observed (Supplementary Figure S2). Furthermore, the results were not driven by single subject (see individual subject results and Jackknife test in Supplementary Figure S4).

Therefore, different task demands (global or local task) on the same global/local compound stimuli induced different rhythms in the corresponding behavioral performances. Global processing is associated with a slower rhythm (i.e., alpha-band) whereas local processing is mediated via a relatively faster rhythm (i.e., beta-band). Importantly, the frequency-based dissociation of global/local perception is consistent with previous neuroimaging studies (Romei et al., 2011; Smith et al., 2006), but here newly demonstrated in behavioral performance.

Global-alpha correlates with global precedence effect

After demonstrating the coexistence of traditional GPE profiles (Figure 1B, 2B) and an additional alpha/beta oscillatory pattern (Figure 2C, 2D) in the same global/local behavioral performance, we next investigated whether the two behavioral components (i.e.,

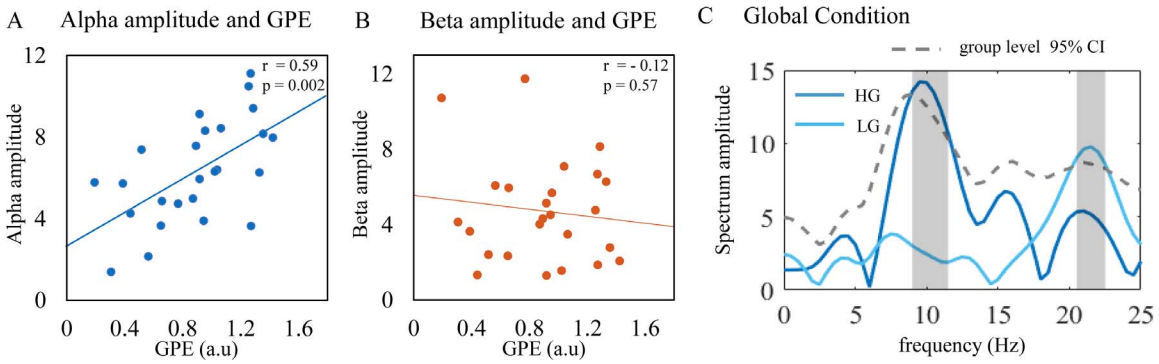

Figure 3. Association between Global-alpha and global precedence effect (GPE). (A) Correlation between the amplitude of Global-alpha behavioral oscillation and the global precedence effect (GPE) across all participants ($n = 25$). (B) Correlation between the amplitude of Local-beta behavioral oscillation and GPE across all participants. Note the significant positive relationship between Global-alpha and GPE (blue) and no significant relationship between Local-beta and GPE (red), suggesting a strong association between Global-alpha and the classical GPE. (C) Subjects were divided, based on their overall GPEs, into two groups: high GPE group (HG group: dark blue) and low GPE group (LG group: light blue), and the same analysis was performed on the two groups separately. Amplitude spectrum of the global task for the HG (dark blue) and LG (light blue) groups was a function of frequency (0–25 Hz). To examine the statistical significance between the HG and LG groups, we randomly selected 12 subjects from all the subjects (across HG and LG groups) and performed the same spectrum analysis on each selection. We repeated this process for 2,000 times, from which the 95% CI for the amplitude spectrum as a function of frequency could be obtained (dashed line) and was compared to the amplitude spectrum of the HG and LG groups. Note that the HG group (dark blue) showed stronger Global-alpha, whereas the LG group (light blue) showed enhanced Local-beta (gray shades).

classical GPE and the new alpha/band-band behavioral oscillations) would exhibit any correlations between each other. To address the issue, we calculated the classical GPE (overall RT_{local} − overall RT_{global}; see Figure 1B) and extracted the alpha-band and the beta-band amplitude for the global- and local-task behavioral performance respectively (i.e., "Global-alpha" and "Local-beta", see Figure 2D) in each subject. We then performed a subject-by-subject correlation analysis between the behavioral oscillatory components (Global-alpha and Local-beta) and the classical GPE. As shown in Figure 3A, significant correlation was found between Global-alpha and GPE (Pearson's correlation, $N = 25$, $r = 0.59$, $p = 0.002$), suggesting that subjects with lager alpha-band in global behavioral performance (i.e., stronger Global-alpha) showed larger classical global advantage (i.e., GPE). On the other hand, the Local-beta did not correlate with GPE significantly ($r = -0.12$, $p = 0.57$, Figure 3B), indicating that only the oscillatory component engaged in global task (Global-alpha), rather than the one involved in local task (Local-beta), is closely connected to the classical global precedence effect (similar results were obtained when using median RT or single-trial fitting approach, see Supplementary Figure S3).

To further confirm the relationship between Global-alpha and GPE, we next divided all the subjects into two groups based on their overall GPE (high GPE group and low GPE group). High GPE group/HG, $N = 12$, mean = 76.67 ms, $SD = 29.41$ ms; low GPE group/LG, $N = 12$, mean = 39.41 ms, $SD = 25.38$ ms; independent sample t test for HG and LG, $t(22) = 6.99$, Cohen's $d = 1.35$, $p < 0.001$. We then performed the spectrum analyses on the detrended behavioral time courses for each group separately. Figure 3C shows the spectrum profiles of the global task for the HG (dark blue) and LG (light blue) groups. As expected, the HG group (dark blue) showed significant alpha-band behavioral oscillations, consistent with the correlation results (Figure 3A). However, interestingly, the LG group (light blue) during the global task, in addition to displaying decreased alpha-band (not significant), showed activations that somewhat shifted to the beta-band, the frequency range for local processing. To further examine the statistical significance between the HG and LG groups, we randomly selected 12 subjects from all the subjects (across HG and LG group) and performed the same spectrum analysis on each selection. We repeated this process for 2,000 times, from which the group level 95% CI for the amplitude spectrum as a function of frequency could be calculated. Compared to the 95% CI of amplitude spectrum (dashed line, Figure 3C), it is clear that the HG group (dark blue) showed significant alpha-band activations, whereas the LG group (light blue) showed significant beta-band activations.

Taken together, our results demonstrate that the time-resolved global/local behavioral traces (Figure 2A) consist of two concurrent components. One is the well-established GPE (Figure 2B), a classical phenomenon in global/local processing (1). In addition and most importantly, we observed a new temporal

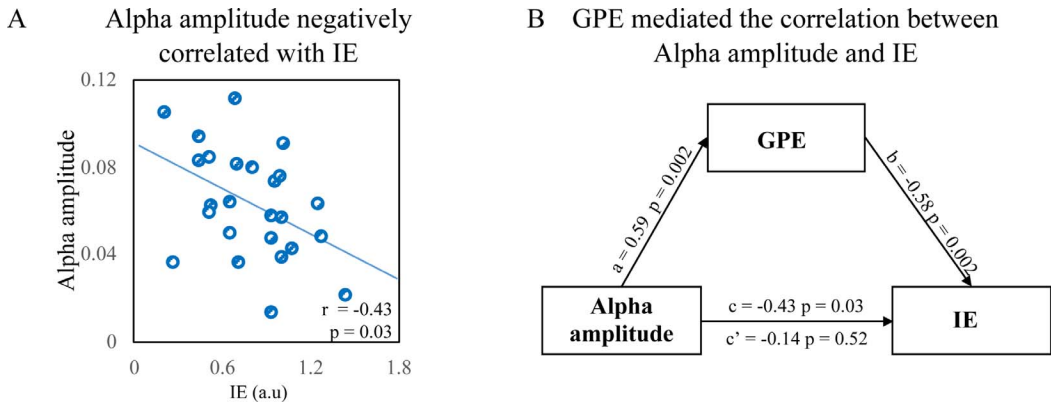

Figure 4. Relationship among interference effect (IE), Global-alpha, and global precedence effect (GPE). (A) Correlation between the amplitude of Global-alpha behavioral oscillation and the interference effect (IE) across all participants ($n = 25$). Note that Global-alpha is negatively correlated with IE, supporting the concept that the stronger the global-alpha is, the less interference influence the incongruent local feature would exert on global processing. (B) Mediation analysis on the Global-alpha, global precedence effect (GPE), and IE, and the results indicate that GPE mediates the negative correlation between Global-alpha and IE. In other words, stronger Global-alpha oscillatory activation is accompanied by decreased IE (local interference on global processing), and this process is essentially mediated by the GPE (i.e., global advantage over local processing).

component—a behavioral oscillatory pattern that occurs in alpha-band and beta-band for global and local tasks respectively. Furthermore, the Global-alpha component is essentially correlated with the classical GPE such that the larger the Global-alpha, the stronger the GPE would be.

Interference effect, Global-alpha, and global precedence effect

In addition to GPE, whether the global and local properties are congruent (C) or incongruent (IC) with each other is another factor that would affect the global/local behavioral performance. Interference effect (IE), referring to faster RTs for congruent over incongruent compound stimuli, has been shown in the overall behavioral performance (Figure 1B). We thus further examined the relationship between IE (overall $RT_{IC\text{-}Global}$ − overall $RT_{C\text{-}Global}$; see Figure 1B) and the Global-alpha activations. As shown in Figure 4A, these two variables displayed a significant negative correlation (Pearson's correlation, $N = 25$, $r = -0.43$, $p = 0.03$), supporting that the larger the global-alpha is, the less interference influence the incongruent local feature would exert on global processing. In other words, global perception would receive little interferences from local properties during stronger Global-alpha activations (larger amplitude), again confirming a key function of Global-alpha in global analysis.

We further performed a mediation analysis to examine how the Global-alpha influences IE and the possible involvement of GPE. As shown in Figure 4B, the Global-alpha amplitude was correlated with both GPE ($\beta_a = -0.59$, $p = 0.002$) and IE ($\beta_c = 0.43$, $p = 0.03$). Importantly, Global-alpha amplitude was no longer related to IE when controlling GPE ($\beta_{c'} = -0.14$, $p = 0.52$), and the indirect influence from GPE on the correlation between Global-alpha amplitude and IE was significant (bootstrapping, *indirect effect* $= -0.04$, *confidence interval*: $-0.07 \sim -0.01$). The results support that stronger Global-alpha oscillatory activation (larger amplitude) was accompanied by decreased IE (local interference effect on global processing), and this process was mediated by the GPE (i.e., global fast over local processing).

Discussion

We used a time-resolved psychophysical approach to assess the fine temporal structure of global/local processing in behavior performance. First, we replicated the classic GPE in the slowly developing trend. Second, after removing the slow trend, the global and local reaction time shows distinctive oscillations in the alpha (~10 Hz) and beta bands (~20 Hz) respectively ("Global-alpha" and "Local-beta"), consistent with previous neuroimaging findings (Romei et al., 2011; Smith et al., 2006). Importantly, the Global-alpha activities are strongly correlated with the classical global/local perception effects (i.e., GPE and IE). Specifically, the stronger the Global-alpha activations, the larger the typical global precedence effect is, and the less interference the global processing would receive from incongruent local features. To our knowledge, our findings constitute the first behavioral evidence advocating the hypothesis that central function of dissociated neuronal oscillations in mediating global and local

analysis of visual inputs. It is well acknowledged that global properties are processed faster than local ones, and here we replicated the classical GPE in the slow trends of the time-resolved behavioral courses. Processing of global and local features has been found to be associated with distinct neural networks that are characterized by different temporal dynamics. Specifically, global property is mediated via the rapid magnocellular pathway and frontal-parietal networks, whereas the local feature is processed through the relatively slow parvocellular pathway and temporal-parietal network (Coleman et al., 2009; Leaver et al., 2015; Wutz, Loonis, Roy, Donoghue, & Miller, 2018).

Importantly, after removing the slow trends, we have revealed dissociated behavioral oscillations for global and local processing respectively—the Global-alpha and Local-beta. The results are commensurate with previous neurophysiological findings, which suggest that the low-frequency (i.e., theta/alpha-band) and high-frequency (i.e., beta-band) neuronal activations play distinct roles in global and local processing (Romei et al., 2011; Smith et al., 2006). Why do slow rhythms (e.g., theta, alpha) mediate global perception whereas faster rhythms (e.g., beta) engage in local processing? A possible interpretation is that global analysis in principle would require integration and coordination over more brain regions to overcome fluctuating noise, and thus a longer temporal integration window would be more appropriate. Local feature analysis, in contrast, would be within small and specific brain regions as well as being able to track momentary changes, for which a high-frequency rhythm would be more suitable (e.g., Kloosterman et al., 2015; von Stein & Sarnthein, 2000). Interestingly, it has been recently posited that different stimulus attributes could be encoded at distinct time scales concurrently, and this "temporal multiplexing" strategy would enable the brain to form an information-rich and stable representation of the environment (Palva & Palva, 2007; Panzeri, Brunel, Logothetis, & Kayser, 2010; Wutz et al., 2018). Thus, neural codes operating at different temporal scales (i.e., long and short windows, corresponding to low- and high-frequencies) for global and local properties would constitute an efficient mechanism to represent complementary features and enhance the coding capacity of the system.

Most importantly, our results show that the Global-alpha activations are strongly correlated with the classical global/local perception effect (i.e., GPE and IE). Specifically, the larger the alpha-band activations, the stronger the global advantage effect is (larger GPE), and the less disruptions the global perception receives from incongruent local features (smaller IE). Mediation analysis further supports the key role of the Global-alpha in driving the whole process. Previous TMS study has provided convincing evidence supporting the causal role of neuronal oscillations in global/local processing (Romei et al., 2011), and our results significantly extend previous findings by establishing a direct relationship between neuronal oscillations, particularly the global-alpha rhythms, and the classical global advantage effect. Furthermore and interestingly, our results demonstrate that the low-GPE subject group, when performing a global task, showed a shift to beta-band frequency range, the rhythm for local analysis (Local-beta). Thus, when subjects employ an unsuitable rhythm (e.g., beta-band here) in global tasks, they would fail to process global attributes at appropriate temporal scales (e.g., alpha-band here), resulting in the lack of global advantage effect in their behavioral performances.

Previous studies have shown that global processing is mediated by the theta-band response (Romei et al., 2011; Smith et al., 2006), whereas here we only observed alpha-band activation in global task. Although consistent with each other in low-frequency for global analysis, the frequency distinction might be due to different stimuli employed in the task. Specifically, previous studies used high-level objects, such as face or letter, whereas here we employed low-level stimuli and subjects were instructed to determine their orientations. It is known that identifying the orientation of a simple stimulus (e.g., arrow-like figure) might involve activations of early visual areas while recognizing the identity of a high-level object (e.g., face or letter) might depend on high ventral areas that are associated with theta-band neuronal oscillations (Drewes et al., 2015; Ronconi, Oosterhof, Bonmassar, & Melcher, 2017; Wang & Luo, 2017); also see the review by Mitchell, McNaughton, Flanagan, and Kirk (2008).

Another interpretation for the frequency difference between global and local tasks might be the saliency difference between global and local features. Specifically, the global configuration of the figure would be more salient than the local features, and therefore the global task would involve stronger alpha-band activities (Jensen, Bonnefond, & VanRullen, 2012). However, in our experiment, the same compound stimulus was used for global and local tasks, and both tasks were actually balanced in saliency. If alpha-band activities were associated with saliency extraction, we would expect alpha-band activation for both global and local tasks. Meanwhile, we did not observe alpha-band responses in local task at all, supporting that it was the task rather than the saliency information that could account for the results. Furthermore, alpha-band neuronal oscillation has been shown to play an inhibitory function in many cognitive processes (see review by Foxe & Snyder, 2011), and linking to our results here, the observed "Global-alpha" might be explained by stronger suppression of local analysis during global task. We, however, do not think this

could account for the results because, in both global and local tasks, there would be task-irrelevant features needed to be inhibited and if Alpha-band indexed an inhibitory process here, we would expect alpha-band response in local task as well, which was not the case here. Moreover, our "Global-alpha" findings are also consistent with recent studies showing that alpha-band is more related to detection bias rather than visual sensitivity (Benwell, Keitel, Harvey, Gross, & Thut, 2017; Benwell, Tagliabue, et al., 2017; Iemi, Chaumon, Crouzet, & Busch, 2017; Samaha, Iemi, & Postle, 2017).

A possible concern is that the observed different frequencies for global and local tasks might be due to different eye movements. Previous monkey electrophysiological recordings show that eye movements are accompanied by complex changes in oscillatory activity at various frequencies (e.g., Bosman, Womelsdorf, Desimone, & Fries, 2009; Brunet et al., 2015; Hoffman et al., 2013; Ito, Maldonado, Singer, & Grun, 2011; Jutras, Fries, & Buffalo, 2013; Lowet et al., 2018). Behavioral oscillations have also been shown to be synchronized with saccadic execution (Benedetto & Morrone, 2017; Hogendoorn, 2016; Wutz et al., 2016) or occur after a microsaccade movement (Bellet, Chen, & Hafed, 2017). Future studies are needed to combine eye movement recordings with time-resolved behavioral measurement to understand their interactions.

Finally, there a contradiction seems to exist between the classical GPE and the slow/fast rhythms for global/local processing findings. Specifically, on the one hand, the global features are perceived faster than local ones (i.e., GPE), but on the other hand, the global properties are processed in a slow-paced neural rhythm compared to the local analysis. The inconsistency could be possibly interpreted and reconciled in terms of the "Reversed hierarchical theory" (RHT), which proposes that although feedforward processing is along a simple-to-complex hierarchy (e.g., from local to global processing), the conscious perception begins at the hierarch's top, following a reverse hierarchical course (e.g., from global to local perception; Hochstein & Ahissar, 2002; Moratti, Mendez-Bertolo, Del-Pozo, & Strange, 2014). According to this theory, local analysis that is presumably mediated by fast rhythms in local regions would be performed prior to global analysis, which relies on slow neuronal oscillations to coordinate information integration over large numbers of regions and long temporal windows. Meanwhile, due to the conscious perception that follows a reverse hierarchical direction, the global properties would be perceived faster than local attributes, resulting in the global precedence effect (GPE). In other words, distinct neuronal rhythms could mediate the global/local analysis along the feedforward passage whereas the overall global advantage effect occurs as a result of reverse hierarchical routines. Previous studies have provided neural evidence supporting this global-to-local, coarse-to-fine course in visual perception along the reverse hierarchical routines (Bar et al., 2006; Epshtein, Lifshitz, & Ullman, 2008; Kahneman, Treisman, & Gibbs, 1992; Liu, Wang, Zhou, Ding, & Luo, 2017; von der Heydt, 2015; Wagemans et al., 2012; Xu & Chun, 2007).

Keywords: global precedence effect, alpha-band, beta-band, behavioral oscillation, time-resolved psychophysics

Acknowledgments

We thank Dr. Nai Ding and Fan Ying for helpful comments.

This work was supported by National Nature Science Foundation of China Grants 31522027 and 31571115 to HL, Beijing Municipal Science & Technology Commission Grants Z181100001518002 to HL, and the project was funded by China Postdoctoral Science Foundation Grants 2018M641045 to LL.

Commercial relationships: none.
Corresponding authors: Ling Liu; Huan Luo.
Email: ling.liu@pku.edu.cn; huan.luo@pku.edu.cn.
Address: School of Psychological and Cognitive Sciences, Peking University, Beijing, China.

References

Bar, M., Kassam, K. S., Ghuman, A. S., Boshyan, J., Schmid, A. M., Dale, A. M., . . . Halgren, E. (2006). Top-down facilitation of visual recognition. *Proceedings of the National Academy of Sciences, USA*, *103*(2), 449–454, https://doi.org/10.1073/pnas.0507062103.

Bellet, J., Chen, C. Y., & Hafed, Z. M. (2017). Sequential hemifield gating of alpha- and beta-behavioral performance oscillations after microsaccades. *Journal of Neurophysiology*, *118*(5), 2789–2805, https://doi.org/10.1152/jn.00253.2017.

Benedetto, A., & Morrone, M. C. (2017). Saccadic suppression is embedded within extended oscillatory modulation of sensitivity. *Journal of Neuroscience*, *37*(13), 3661–3670, https://doi.org/10.1523/JNEUROSCI.2390-16.2016.

Benwell, C. S. Y., Keitel, C., Harvey, M., Gross, J., & Thut, G. (2017). Trial-by-trial co-variation of pre-stimulus EEG alpha power and visuospatial bias reflects a mixture of stochastic and deterministic

effects. *European Journal of Neuroscience*, *48*(7), 2566–2584, https://doi.org/10.1111/ejn.13688.

Benwell, C. S. Y., Tagliabue, C. F., Veniero, D., Cecere, R., Savazzi, S., & Thut, G. (2017). Prestimulus EEG power predicts conscious awareness but not objective visual performance. *eNeuro*, *4*(6):e0182-17.2017, 1–17, https://doi.org/10.1523/ENEURO.0182-17.2017.

Bosman, C. A., Womelsdorf, T., Desimone, R., & Fries, P. (2009). A microsaccadic rhythm modulates gamma-band synchronization and behavior. *Journal of Neuroscience*, *29*(30), 9471–9480, https://doi.org/10.1523/JNEUROSCI.1193-09.2009.

Brunet, N., Bosman, C. A., Roberts, M., Oostenveld, R., Womelsdorf, T., De Weerd, P., & Fries, P. (2015). Visual cortical gamma-band activity during free viewing of natural images. *Cerebral Cortex*, *25*(4), 918–926, https://doi.org/10.1093/cercor/bht280.

Coleman, M. J., Cestnick, L., Krastoshevsky, O., Krause, V., Huang, Z., Mendell, N. R., & Levy, D. L. (2009). Schizophrenia patients show deficits in shifts of attention to different levels of global-local stimuli: Evidence for magnocellular dysfunction. *Schizophrenia Bulletin*, *35*(6), 1108–1116, https://doi.org/10.1093/schbul/sbp090.

Drewes, J., Zhu, W., Wutz, A., & Melcher, D. (2015). Dense sampling reveals behavioral oscillations in rapid visual categorization. *Scientific Reports*, *5*, 16290, https://doi.org/10.1038/srep16290.

Epshtein, B., Lifshitz, I., & Ullman, S. (2008). Image interpretation by a single bottom-up top-down cycle. *Proceedings of the National Academy of Sciences, USA*, *105*(38), 14298–14303, https://doi.org/10.1073/pnas.0800968105.

Fiebelkorn, I. C., Foxe, J. J., Butler, J. S., Mercier, M. R., Snyder, A. C., & Molholm, S. (2011). Ready, set, reset: Stimulus-locked periodicity in behavioral performance demonstrates the consequences of cross-sensory phase reset. *Journal of Neuroscience*, *31*(27), 9971–9981, https://doi.org/10.1523/JNEUROSCI.1338-11.2011.

Fiebelkorn, I. C., Pinsk, M. A., & Kastner, S. (2018). A Dynamic Interplay within the frontoparietal network underlies rhythmic spatial attention. *Neuron*, *99*(4), 842–853 e848, https://doi.org/10.1016/j.neuron.2018.07.038.

Fiebelkorn, I. C., Saalmann, Y. B., & Kastner, S. (2013). Rhythmic sampling within and between objects despite sustained attention at a cued location. *Current Biology*, *23*(24), 2553–2558, https://doi.org/10.1016/j.cub.2013.10.063.

Flevaris, A. V., Bentin, S., & Robertson, L. C. (2011). Attentional selection of relative SF mediates global versus local processing: Evidence from EEG. *Journal of Vision*, *11*(7):11, 1–12, https://doi.org/10.1167/11.7.11. [PubMed] [Article]

Foxe, J. J., & Snyder, A. C. (2011). The role of Alpha-band brain oscillations as a sensory suppression mechanism during selective attention. *Frontiers in Psychology*, *2*, 154, https://doi.org/10.3389/fpsyg.2011.00154.

Hayes, A. F. (2018). *Introduction to mediation, moderation, and conditional process analysis: A regression-based approach* (2nd ed.). New York, NY: Guilford Press.

Ho, H. T., Leung, J., Burr, D. C., Alais, D., & Morrone, M. C. (2017). Auditory sensitivity and decision criteria oscillate at different frequencies separately for the two ears. *Current Biology*, *27*(23), 3643–3649 e3643, https://doi.org/10.1016/j.cub.2017.10.017.

Hochstein, S., & Ahissar, M. (2002). View from the top: Hierarchies and reverse hierarchies in the visual system. *Neuron*, *36*(5), 791–804.

Hoffman, K. L., Dragan, M. C., Leonard, T. K., Micheli, C., Montefusco-Siegmund, R., & Valiante, T. A. (2013). Saccades during visual exploration align hippocampal 3–8 Hz rhythms in human and non-human primates. *Frontiers in Systems Neuroscience*, *7*(43), 1–10, https://doi.org/10.3389/fnsys.2013.00043.

Hogendoorn, H. (2016). Voluntary saccadic eye movements ride the attentional rhythm. *Journal of Cognitive Neuroscience*, *28*(10), 1625–1635, https://doi.org/10.1162/jocn_a_00986.

Huang, Y., Chen, L., & Luo, H. (2015). Behavioral oscillation in priming: Competing perceptual predictions conveyed in alternating theta-band rhythms. *Journal of Neuroscience*, *35*(6), 2830–2837, https://doi.org/10.1523/JNEUROSCI.4294-14.2015.

Iemi, L., Chaumon, M., Crouzet, S. M., & Busch, N. A. (2017). Spontaneous Neural Oscillations Bias Perception by Modulating Baseline Excitability. *Journal of Neuroscience*, *37*(4), 807–819, https://doi.org/10.1523/JNEUROSCI.1432-16.2016.

Ito, J., Maldonado, P., Singer, W., & Grun, S. (2011). Saccade-related modulations of neuronal excitability support synchrony of visually elicited spikes. *Cerebral Cortex*, *21*(11), 2482–2497, https://doi.org/10.1093/cercor/bhr020.

Jensen, O., Bonnefond, M., & VanRullen, R. (2012). An oscillatory mechanism for prioritizing salient unattended stimuli. *Trends in Cognitive Sciences*,

16(4), 200–206, https://doi.org/10.1016/j.tics.2012.03.002.

Jutras, M. J., Fries, P., & Buffalo, E. A. (2013). Oscillatory activity in the monkey hippocampus during visual exploration and memory formation. *Proceedings of the National Academy of Sciences, USA*, *110*(32), 13144–13149, https://doi.org/10.1073/pnas.1302351110.

Kahneman, D., Treisman, A., & Gibbs, B. J. (1992). The reviewing of object files: Object-specific integration of information. *Cognitive Psychology*, *24*(2), 175–219.

Kloosterman, N. A., Meindertsma, T., Hillebrand, A., van Dijk, B. W., Lamme, V. A., & Donner, T. H. (2015). Top-down modulation in human visual cortex predicts the stability of a perceptual illusion. *Journal of Neurophysiology*, *113*(4), 1063–1076, https://doi.org/10.1152/jn.00338.2014.

Landau, A. N., & Fries, P. (2012). Attention samples stimuli rhythmically. *Current Biology*, *22*(11), 1000–1004, https://doi.org/10.1016/j.cub.2012.03.054.

Leaver, E. E., Low, K. A., DiVacri, A., Merla, A., Fabiani, M., & Gratton, G. (2015). The devil is in the detail: Brain dynamics in preparation for a global-local task. *Journal of Cognitive Neuroscience*, *27*(8), 1513–1527, https://doi.org/10.1162/jocn_a_00800.

Liu, L., Wang, F., Zhou, K., Ding, N., & Luo, H. (2017). Perceptual integration rapidly activates dorsal visual pathway to guide local processing in early visual areas. *PLoS Biology*, *15*(11), e2003646, https://doi.org/10.1371/journal.pbio.2003646.

Lowet, E., Gomes, B., Srinivasan, K., Zhou, H., Schafer, R. J., & Desimone, R. (2018). Enhanced neural processing by covert attention only during microsaccades directed toward the attended stimulus. *Neuron*, *99*(1), 207–214 e203, https://doi.org/10.1016/j.neuron.2018.05.041.

Maris, E., & Oostenveld, R. (2007). Nonparametric statistical testing of EEG- and MEG-data. *Journal of Neuroscience Methods*, *164*(1), 177–190, https://doi.org/10.1016/j.jneumeth.2007.03.024.

Mitchell, D. J., McNaughton, N., Flanagan, D., & Kirk, I. J. (2008). Frontal-midline theta from the perspective of hippocampal "theta." *Progress in Neurobiology*, *86*(3), 156–185, https://doi.org/10.1016/j.pneurobio.2008.09.005.

Moratti, S., Mendez-Bertolo, C., Del-Pozo, F., & Strange, B. A. (2014). Dynamic gamma frequency feedback coupling between higher and lower order visual cortices underlies perceptual completion in humans. *Neuroimage*, *86*, 470–479, https://doi.org/10.1016/j.neuroimage.2013.10.037.

Navon, D. (1977). Forest before trees: The precedence of global features in visual perception. *Cognitive Psychology*, *9*(3), 353–383, https://doi.org/10.1016/0010-0285(77)90012-3.

Palva, S., & Palva, J. M. (2007). New vistas for alpha-frequency band oscillations. *Trends in Neurosciences*, *30*(4), 150–158, https://doi.org/10.1016/j.tins.2007.02.001.

Panzeri, S., Brunel, N., Logothetis, N. K., & Kayser, C. (2010). Sensory neural codes using multiplexed temporal scales. *Trends in Neurosciences*, *33*(3), 111–120, https://doi.org/10.1016/j.tins.2009.12.001.

Romei, V., Driver, J., Schyns, P. G., & Thut, G. (2011). Rhythmic TMS over parietal cortex links distinct brain frequencies to global versus local visual processing. *Current Biology*, *21*(4), 334–337, https://doi.org/10.1016/j.cub.2011.01.035.

Romei, V., Thut, G., Mok, R. M., Schyns, P. G., & Driver, J. (2012). Causal implication by rhythmic transcranial magnetic stimulation of alpha frequency in feature-based local vs. global attention. *European Journal of Neuroscience*, *35*(6), 968–974, https://doi.org/10.1111/j.1460-9568.2012.08020.x.

Ronconi, L., Oosterhof, N. N., Bonmassar, C., & Melcher, D. (2017). Multiple oscillatory rhythms determine the temporal organization of perception. *Proceedings of the National Academy of Sciences, USA*, *114*(51), 13435–13440, https://doi.org/10.1073/pnas.1714522114.

Samaha, J., Iemi, L., & Postle, B. R. (2017). Prestimulus alpha-band power biases visual discrimination confidence, but not accuracy. *Consciousness and Cognition*, *54*, 47–55, https://doi.org/10.1016/j.concog.2017.02.005.

Smith, M. L., Gosselin, F., & Schyns, P. G. (2006). Perceptual moments of conscious visual experience inferred from oscillatory brain activity. *Proceedings of the National Academy of Sciences, USA*, *103*(14), 5626–5631, https://doi.org/10.1073/pnas.0508972103.

Song, K., Meng, M., Chen, L., Zhou, K., & Luo, H. (2014). Behavioral oscillations in attention: Rhythmic alpha pulses mediated through theta band. *Journal of Neuroscience*, *34*(14), 4837–4844, https://doi.org/10.1523/JNEUROSCI.4856-13.2014.

Tomassini, A., Ambrogioni, L., Medendorp, W. P., & Maris, E. (2017). Theta oscillations locked to intended actions rhythmically modulate perception. *Elife*, *6*:e25618, https://doi.org/10.7554/eLife.25618.

Tomassini, A., Spinelli, D., Jacono, M., Sandini, G., & Morrone, M. C. (2015). Rhythmic oscillations of

visual contrast sensitivity synchronized with action. *Journal of Neuroscience*, *35*(18), 7019–7029, https://doi.org/10.1523/JNEUROSCI.4568-14.2015.

von der Heydt, R. (2015). Figure-ground organization and the emergence of proto-objects in the visual cortex. *Frontiers in Psychology*, *6*, 1695, https://doi.org/10.3389/fpsyg.2015.01695.

von Stein, A., & Sarnthein, J. (2000). Different frequencies for different scales of cortical integration: From local gamma to long range alpha/theta synchronization. *International Journal of Psychophysiology*, *38*(3), 301–313.

Wagemans, J., Feldman, J., Gepshtein, S., Kimchi, R., Pomerantz, J. R., van der Helm, P. A., & van Leeuwen, C. (2012). A century of Gestalt psychology in visual perception: II. Conceptual and theoretical foundations. *Psychological Bulletin*, *138*(6), 1218–1252, https://doi.org/10.1037/a0029334.

Wang, Y. Y., & Luo, H. (2017). Behavioral oscillation in face priming: Prediction about face identity is updated at a theta-band rhythm. *Progress in Brain Research*, *236*, 211–224, https://doi.org/10.1016/bs.pbr.2017.06.008.

Wutz, A., Loonis, R., Roy, J. E., Donoghue, J. A., & Miller, E. K. (2018). Different levels of category abstraction by different dynamics in different prefrontal areas. *Neuron*, *97*(3), 716–726 e718, https://doi.org/10.1016/j.neuron.2018.01.009.

Wutz, A., Muschter, E., van Koningsbruggen, M. G., Weisz, N., & Melcher, D. (2016). Temporal integration windows in neural processing and perception aligned to saccadic eye movements. *Current Biology*, *26*(13), 1659–1668, https://doi.org/10.1016/j.cub.2016.04.070.

Xu, Y., & Chun, M. M. (2007). Visual grouping in human parietal cortex. *Proceedings of the National Academy of Sciences, USA*, *104*(47), 18766–18771, https://doi.org/10.1073/pnas.0705618104.